

Polymer-stabilized blue phase liquid crystals: a tutorial [Invited]

Jin Yan and Shin-Tson Wu*

College of Optics and Photonics, University of Central Florida, Orlando, FL 32816, USA

*swu@mail.ucf.edu

Abstract: Blue phase liquid crystals exhibit several attractive features, such as self-assembled three-dimensional cubic structures, optically-isotropic in the voltage-off state, no need for alignment layers, and submillisecond response time. This tutorial gives step-by-step introduction on basic blue-phase materials and properties, monomers and polymerization processes, and key device performance criteria for display and photonics applications.

©2011 Optical Society of America

OCIS codes: (160.3710) Liquid crystals; (160.5470) Polymers.

References and links

1. F. Reinitzer, "Beiträge zur Kenntniss des Cholesterins," *Monatsh. Chem.* **9**(1), 421–441 (1888).
2. A. Saupe, "On molecular structure and physical properties of thermotropic liquid crystals," *Mol. Cryst. Liq. Cryst. (Phila. Pa.)* **7**(1), 59–74 (1969).
3. S. A. Brazovskii and S. G. Dmitriev, "Phase transitions in cholesteric liquid crystals," *Zh. Eksp. Teor. Fiz.* **69**, 979–989 (1975).
4. R. M. Hornreich and S. Shtrikman, *Liquid Crystals of One- and Two- Dimensional Order* (Springer-Verlag, Berlin, 1980).
5. S. Meiboom, J. P. Sethna, W. P. Anderson, and W. F. Brinkman, "Theory of the blue phase cholesteric liquid crystals," *Phys. Rev. Lett.* **46**(18), 1216–1219 (1981).
6. E. Dubois-Violette and B. Pansu, "Frustration and related topology of blue phases," *Mol. Cryst. Liq. Cryst. (Phila. Pa.)* **165**, 151–182 (1988).
7. P. P. Crooker, *Chirality in Liquid Crystals* (Springer, New York, 2001), Chap. 7.
8. D. L. Johnson, J. H. Flack, and P. P. Crooker, "Structure and properties of the cholesteric blue phases," *Phys. Rev. Lett.* **45**(8), 641–644 (1980).
9. P. E. Cladis, T. Garel, and P. Pieranski, "Kossel diagrams show electric-field-induced cubic-tetragonal structural transition in frustrated liquid-crystal blue phases," *Phys. Rev. Lett.* **57**(22), 2841–2844 (1986).
10. R. J. Miller and H. F. Gleeson, "Order parameter measurements from the Kossel diagrams of the liquid-crystal blue phases," *Phys. Rev. E Stat. Phys. Plasmas Fluids Relat. Interdiscip. Topics* **52**(5), 5011–5016 (1995).
11. H. S. Kitzerow, H. Schmid, A. Ranft, G. Heppke, R. A. M. Hikmet, and J. Lub, "Observation of blue phases in chiral networks," *Liq. Cryst.* **14**(3), 911–916 (1993).
12. H. Kikuchi, M. Yokota, Y. Hisakado, H. Yang, and T. Kajiyama, "Polymer-stabilized liquid crystal blue phases," *Nat. Mater.* **1**(1), 64–68 (2002).
13. H. J. Coles and M. N. Pivnenko, "Liquid crystal 'blue phases' with a wide temperature range," *Nature* **436**(7053), 997–1000 (2005).
14. H. Kikuchi, *Liquid Crystalline Blue Phases* (Springer Berlin / Heidelberg, 2008), pp. 99–117.
15. G. Heppke, H.-S. Kitzerow, and M. Krumrey, "Electric field induced variation of the refractive index in cholesteric blue phases," *Mol. Cryst. Liq. Cryst. Lett.* **2**, 59–65 (1985).
16. J. Yan, L. Rao, M. Jiao, Y. Li, H. C. Cheng, and S. T. Wu, "Polymer-stabilized optically-isotropic liquid crystals for next-generation display and photonics applications," *J. Mater. Chem.* **21**(22), 7870–7877 (2011).
17. G. Heppke, B. Jérôme, H.-S. Kitzerow, and P. Pieranski, "Electrostriction of the cholesteric blue phases BPI and BPII in mixtures with positive dielectric anisotropy," *J. Phys. (France)* **50**(19), 2991–2998 (1989).
18. H. Stegemeyer and F. Porsch, "Electric field effect on phase transitions in liquid-crystalline blue-phase systems," *Phys. Rev. A* **30**(6), 3369–3371 (1984).
19. H.-S. Kitzerow, "The effect of electric fields on blue phases," *Mol. Cryst. Liq. Cryst. (Phila. Pa.)* **202**(1), 51–83 (1991).
20. K. M. Chen, S. Gauza, H. Xianyu, and S. T. Wu, "Hysteresis effects in blue-phase liquid crystals," *J. Disp. Technol.* **6**(8), 318–322 (2010).
21. J. Yan, H. C. Cheng, S. Gauza, Y. Li, M. Jiao, L. Rao, and S. T. Wu, "Extended Kerr effect of polymer-stabilized blue-phase liquid crystals," *Appl. Phys. Lett.* **96**(7), 071105 (2010).
22. J. Yan, M. Jiao, L. Rao, and S. T. Wu, "Direct measurement of electric-field-induced birefringence in a polymer-stabilized blue-phase liquid crystal composite," *Opt. Express* **18**(11), 11450–11455 (2010).

23. T. Seshadri and H. J. Haupt, "Novel ferrocene-based chiral Schiff's base derivative with a twist-grain boundary phase (TGBA) and a blue phase," *Chem. Commun. (Camb.)* **7**(7), 735–736 (1998).
24. J. Buey, P. Espinet, H. S. Kitzerow, and J. Strauss, "Metallomesogens presenting blue phases in a glassy state and in metallomesogen/nematic mixtures," *Chem. Commun. (Camb.)* **5**(5), 441–442 (1999).
25. G. Heppke, D. Krüerke, C. Löhning, D. Löttsch, D. Moro, M. Müller, and H. Sawade, "New chiral discotic triphenylene derivatives exhibiting a cholesteric blue phase and a ferroelectrically switchable columnar mesophase," *J. Mater. Chem.* **10**(12), 2657–2661 (2000).
26. Y. Haseba and T. Kuninobu, "Optically isotropic liquid crystal medium and optical device," U.S. patent 7,722,783 B2 (2010).
27. Z. Ge, S. Gauza, M. Jiao, H. Xianyu, and S. T. Wu, "Electro-optics of polymer-stabilized blue phase liquid crystal displays," *Appl. Phys. Lett.* **94**(10), 101104 (2009).
28. P. R. Gerber, "Electro-optical effects of a small-pitch blue-phase system," *Mol. Cryst. Liq. Cryst. (Phila. Pa.)* **116**(3-4), 197–206 (1985).
29. H. F. Gleeson and H. J. Coles, "Dynamic properties of blue-phase mixtures," *Liq. Cryst.* **5**(3), 917–926 (1989).
30. L. Rao, J. Yan, S. T. Wu, S. Yamamoto, and Y. Haseba, "A large Kerr constant polymer-stabilized blue phase liquid crystal," *Appl. Phys. Lett.* **98**(8), 081109 (2011).
31. M. Wittek, N. Tanaka, M. Bremer, D. Pauluth, K. Tarumi, M. C. Wu, D. M. Song, and S. E. Lee, "New materials for polymer-stabilized blue phase," *SID Int. Symp. Digest Tech. Papers* **42**(1), 292–293 (2011).
32. J. Yan and S. T. Wu, "Effect of polymer concentration and composition on blue-phase liquid crystals," *J. Disp. Technol.* **7**(9), 490–493 (2011).
33. Y. Haseba and H. Kikuchi, "Optically isotropic chiral liquid crystals induced by polymer network and their electro-optical behavior," *Mol. Cryst. Liq. Cryst. (Phila. Pa.)* **470**(1), 1–9 (2007).
34. C. Y. Fan, C. T. Wang, T. H. Lin, F. C. Yu, T. H. Huang, C. Y. Liu, and N. Sugiura, "Hysteresis and residual birefringence free polymer-stabilized blue phase liquid crystal," *SID Int. Symp. Digest Tech. Papers* **42**(1), 213–215 (2011).
35. L. Rao, Z. Ge, S. T. Wu, and S. H. Lee, "Low voltage blue-phase liquid crystal displays," *Appl. Phys. Lett.* **95**(23), 231101 (2009).
36. M. Jiao, Y. Li, and S. T. Wu, "Low voltage and high transmittance blue-phase liquid crystal displays with corrugated electrodes," *Appl. Phys. Lett.* **96**(1), 011102 (2010).
37. H. C. Cheng, J. Yan, T. Ishinabe, and S. T. Wu, "Vertical field switching for blue-phase liquid crystal devices," *Appl. Phys. Lett.* **98**(26), 261102 (2011).
38. L. Rao, J. Yan, S. T. Wu, Y. H. Chiu, H. Y. Chen, C. C. Liang, C. M. Wu, P. J. Hsieh, S. H. Liu, and K. L. Cheng, "Critical field for a hysteresis-free blue-phase liquid crystal device," *J. Disp. Technol.* **7**(12), 627–629 (2011).
39. W. Cao, A. Muñoz, P. Palfy-Muhoray, and B. Taheri, "Lasing in a three-dimensional photonic crystal of the liquid crystal blue phase II," *Nat. Mater.* **1**(2), 111–113 (2002).
40. S. Yokoyama, S. Mashiko, H. Kikuchi, K. Uchida, and T. Nagamura, "Laser emission from a polymer-stabilized liquid-crystalline blue phase," *Adv. Mater. (Deerfield Beach Fla.)* **18**(1), 48–51 (2006).
41. J. Yan, Y. Li, and S. T. Wu, "High-efficiency and fast-response tunable phase grating using a blue phase liquid crystal," *Opt. Lett.* **36**(8), 1404–1406 (2011).
42. Y. H. Lin, H. S. Chen, H. C. Lin, Y. S. Tsou, H. K. Hsu, and W. Y. Li, "Polarizer-free and fast response microlens arrays using polymer-stabilized blue phase liquid crystals," *Appl. Phys. Lett.* **96**(11), 113505 (2010).
43. Y. Li and S. T. Wu, "Polarization independent adaptive microlens with a blue-phase liquid crystal," *Opt. Express* **19**(9), 8045–8050 (2011).
44. C. H. Lin, Y. Y. Wang, and C. W. Hsieh, "Polarization-independent and high-diffraction-efficiency Fresnel lenses based on blue phase liquid crystals," *Opt. Lett.* **36**(4), 502–504 (2011).

1. Introduction

Blue phases (BPs) appear as a highly twisted chiral nematic liquid crystal (LC) cools down from isotropic phase. The most obvious feature of blue phases is selective reflection of incident light. In early investigations, blue phases exhibit blue colors; that is how blue phases got their name. Blue phases are not always blue, however; they may reflect light of other colors, depending on the chirality of the liquid crystals. Another important characteristic of blue phases is frustration. They only exist in such a narrow temperature range (0.5-2K) that further investigation of blue phases' true nature was not pursued for over 80 years ever since the discovery by Reinitzer in 1888 [1]. Not until 1970s, the study of blue phases became popular and tremendous progresses had been made. It was discovered that blue phase is optically isotropic while exhibiting unusually strong optical activity. Based on this phenomenon, Saupé proposed that blue phases have cubic superstructures, which is the most foresighted proposal in the history of blue phase studies [2]. Later, much effort was devoted to explore the structure of blue phases, both experimentally and theoretically [3–10]. There are

up to three types of blue phases: BPI, BPII, and BPIII, in the order of increasing temperature. While BPIII possesses the same symmetry as isotropic phase, BPI and BPII are comprised of double-twist cylinders arranged in cubic lattices, as shown in Figs. 1(a) and 1(c). Inside each cylinder, the LC director rotates spatially about any radius of the cylinder. These double-twist cylinders are then fitted into a three-dimensional structure. However, they cannot fill the full space without defects. Therefore, blue phase is a coexistence of double-twist cylinders and disclinations. Defects occur at the points where the cylinders are in contact, as illustrated in Figs. 1(b) and 1(d). These defects tend to make the structure less stable which in turn results in a narrow temperature range. Although the delicate structures of blue phases greatly attract scientific attentions, their applications are limited by the narrow temperature range.

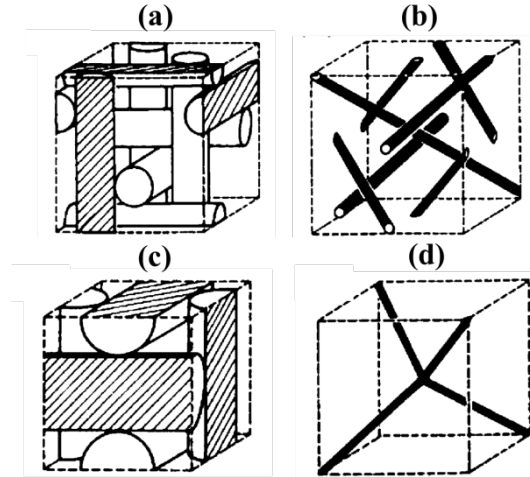


Fig. 1. Cubic structures of BP-I [(a) and (b)] and BP-II [(c) and (d)] filled with double twist cylinders. The black lines in (b) and (d) represent disclination lines.

Several methods have been proposed to widen the temperature range [11–13]. The one that attracts the most interest is the polymer-stabilization method developed by Kikuchi et al. [12]. It is considered that the cross-linked polymer network is selectively concentrated in the disclination lines to stabilize the lattice structure of blue phases. As a result, the temperature range of BPLC has been extended to more than 60K, including room temperature (260-326K). Moreover, the polymer-stabilized blue phase exhibits fast electro-optic switching property. This approach opens a new gateway for display and photonic applications of blue phases. Another wide-temperature-range blue phase liquid crystal is reported by Coles et al. [13]. The large localized flexoelectricity in dimer liquid crystals is considered as the reason for the wide temperature range.

In this tutorial, we give step-by-step introduction on how to prepare and characterize polymer-stabilized BPLCs for photonics and display applications. We emphasize on the optical and electro-optical properties of both pure blue phases and polymer-stabilized blue phases. The optimization of each component in a polymer-stabilized blue phase system is discussed from the application viewpoint. Several examples are given to demonstrate the promising features of the emerging BPLC devices.

2. Blue phase properties

2.1 Bragg Scattering

It is truly remarkable that a liquid can have self-assembled periodic structures, like a photonic crystal. The periodic structure of blue phases results in selective Bragg reflections in the range of light spectrum. It is well-known that selective reflection occurs in cholesteric (chiral

nematic) liquid crystal, the reflection wavelength $\lambda = n \cdot P$, where n is the average refractive index and P is the pitch length. The reflection band is relatively broad with $\Delta\lambda = \Delta n \cdot P$, where Δn is the birefringence of the liquid crystal host. Different from the chiral nematic phase, blue phases do not need any alignment layer and have several reflection wavelengths, corresponding to various crystal planes. The reflection wavelength can be expressed as:

$$\lambda = \frac{2na}{\sqrt{h^2 + k^2 + l^2}}, \quad (1)$$

where n and a denote average refractive index and lattice constant of blue phases, and h , k , and l are the Miller indices. In BPI, the lattice constant corresponds to one pitch length and diffraction peaks appear at (110), (200), and (211), etc. The summation of Miller indices $h + k + l$ is an even number. In BPII, the lattice constant corresponds to half a pitch length and diffraction peaks appear at (100), (110), etc. [14]. The pitch length of a BPLC is slightly different from that of chiral nematic phase. The reflection bandwidth is also much narrower than that of chiral nematic phase. Figure 2 shows the platelet textures of two BPLCs under crossed polarizers. The two photos exhibit different colors because of their different pitch lengths. The multiple colors in one photo correspond to the different crystal planes.

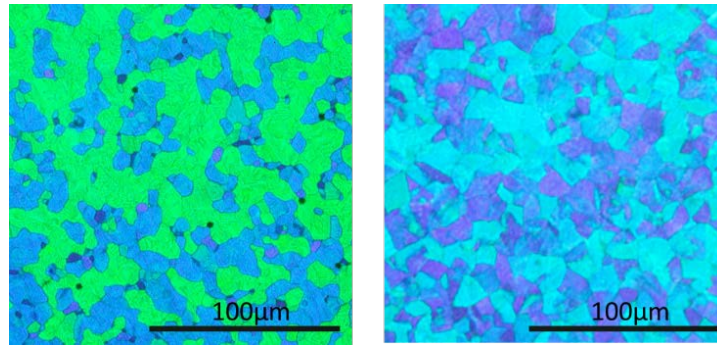


Fig. 2. BPLC platelet textures under polarizing optical microscope with different chiral concentrations.

2.2. Electric field effects

At off-resonance wavelengths, blue phases are optically isotropic. When an electric field (E) is applied, liquid crystal molecules tend to align with the electric field if the dielectric anisotropy $\Delta\epsilon > 0$ (or perpendicular to the electric field if $\Delta\epsilon < 0$). As a result, birefringence is induced. In the low field region, the induced birefringence can be described by Kerr effect as:

$$\Delta n_{ind} = \lambda K E^2, \quad (2)$$

where λ is the wavelength of incident light, K is Kerr constant which depends on wavelength, temperature and driving frequency [15,16]. Kerr effect exhibits a fast response time (<1 ms) because of the short coherent length of BPLC, which is quite attractive for both display and photonics applications. A higher electric field could lead to lattice distortion (electrostriction effect), which results in a shift in the Bragg reflection wavelength according to Eq. (1) [17]. For a sufficiently high electric field, blue phase may transform to new phases, to chiral nematic phases, and ultimately to nematic phases [18,19]. This transition is usually the slowest process (in the order of a few seconds or even longer), which causes undesirable hysteresis or residual birefringence. As a result, the device contrast ratio is degraded.

In a polymer-stabilized blue phase liquid crystal, the polymer network restricts the lattice structure so that color switching behavior is hardly observed [12]. The hysteresis behavior is also different from the pure blue phases [20]. The response time is very fast (<1 ms), which

originates from the Kerr effect. However, Kerr effect is only valid in the low field region because Eq. (2) would lead to divergence if the electric field keeps on increasing. For a finite material system, the induced birefringence should gradually saturate in the high field region once all the molecules have been reoriented. To explain the saturation behavior of the induced birefringence, an extended Kerr effect model has been developed [21,22]:

$$\Delta n = \Delta n_{sat} \left(1 - \exp \left[- \left(\frac{E}{E_s} \right)^2 \right] \right), \quad (3)$$

where Δn_{sat} stands for the saturated induced birefringence and E_s represents the saturation field. As shown in Fig. 3, the measured induced birefringence exhibits a saturation trend which deviates from Kerr effect at high electric field region. The fitting using extend Kerr effect model is quite good in the entire region. This extended Kerr effect not only correctly predicts the saturation phenomenon at high electric field, it is also reduced to Eq. (2) under low field approximation, with Kerr constant $K = \Delta n_{sat}/(\lambda E_s^2)$. Therefore, BPLC materials with high Δn_{sat} and low E_s (e.g., large dielectric anisotropy) are crucial for enhancing Kerr constant, which subsequently lowers the operation voltage.

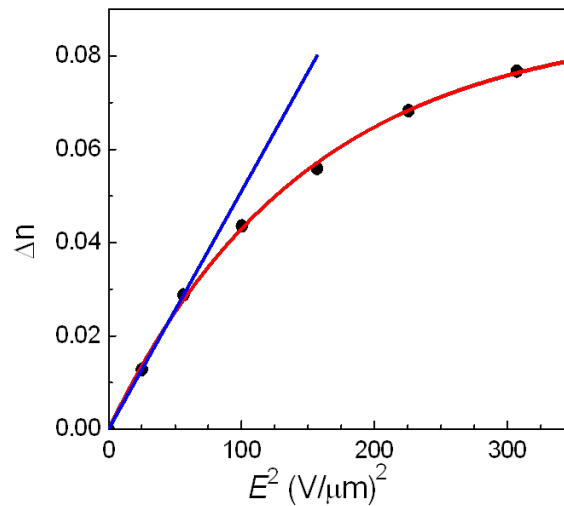


Fig. 3. Measured induced birefringence (dots), linear fitting with Kerr effect (blue line) and fitting with extend Kerr effect model (red line).

3. Polymer-stabilized blue phase materials

Recently, new blue phase materials are developed in various ways [23–25]. Here, we focus on the blue phases induced by incorporating chiral dopants into a nematic LC host. Figure 4 shows some exemplary nematic LC compounds [26], chiral dopants, and monomers.

To make a polymer-stabilized blue phase liquid crystal, a small fraction of monomers (~8%) and photoinitiator (~0.5%) is first added to the blue phase system. A few examples of monomer structures are also included in Fig. 4. Then we control the temperature within the narrow blue phase range to conduct the UV curing process. After UV irradiation, monomers are polymerized to form polymer network which stabilizes the blue phase lattice structures. In this polymer-stabilized self-assembly blue phase system, each material component plays an important role while interacting with each other. The optimization of materials will be discussed later from the application point of view.

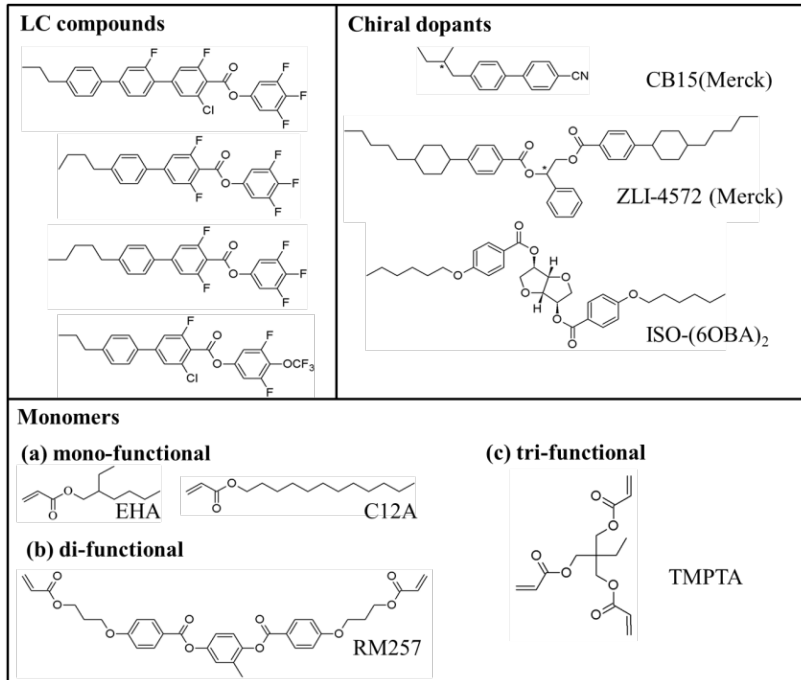


Fig. 4. Examples of nematic liquid crystals, chiral dopants, and monomers.

3.1 Nematic liquid crystals

Nematic liquid crystal host has the highest concentration in polymer-stabilized BPLC material system. Therefore, it plays major role in determining the performance of the system, such as temperature range, driving voltage, and response time. For display and photonics applications, the blue phase temperature range should cover from -40°C to 80°C . To obtain a wide-temperature-range polymer-stabilized BPLC, a nematic LC host should first have a wide nematic range. While the lower temperature limit is less a concern, the higher temperature limit is mainly determined by the clearing point of the nematic LC host. Since other components in the polymer-stabilized BPLC system tend to lower the clearing temperature, it is essential to choose a nematic LC host with clearing temperature $T_c > 80^{\circ}\text{C}$.

The driving voltage of a BPLC device depends on the device structure and the Kerr constant (K) of the material employed. In an IPS device, the on-state voltage (V_{on}) is inversely proportional to the square-root of K [27]. For example, if K increases by 4X then V_{on} would decrease by 2X. Therefore from display application standpoint, the goals for BPLC material development are: 1) to obtain high transmittance ($>80\%$) at low voltage ($V_{on} < 10\text{V}$), 2) to eliminate hysteresis for accurate gray scale control, 3) to minimize residual birefringence for high contrast ratio, 4) to form sturdy BPLC composite with long term stability, and 5) to widen the BP temperature range.

The Kerr constant of a BPLC is determined by several LC parameters as [28]:

$$K \approx \Delta n \cdot \Delta \varepsilon \frac{\varepsilon_o P^2}{k \lambda (2\pi)^2}, \quad (4)$$

where Δn , $\Delta \varepsilon$, and k are the intrinsic birefringence, dielectric anisotropy, and elastic constant of the host LC material, and P is the pitch length. From Eq. (4), to enhance Kerr constant, a liquid crystal with high Δn and large $\Delta \varepsilon$ is highly desirable. Birefringence of a LC is determined by the conjugation length and dielectric anisotropy by the dipole moment. As shown in Fig. 4, the exemplary compounds have 3-4 phenyl rings in order to obtain a high

birefringence and good photo and thermal stabilities. They also have several polar groups for achieving a large $\Delta\epsilon$. Moreover, to keep a high voltage holding ratio in order to avoid image flickering or image sticking, fluoro compounds are preferred. One general shortcoming for having so many polar groups is the increased viscosity. Pitch length also plays an important role in determining the Kerr constant. For display applications, the device should be clear in the visible spectral region. Thus, the Bragg reflection is usually designed to be <400 nm. As a result, the pitch length is normally ~ 200 nm. Such a short pitch length would lead to a fairly high voltage. One possible strategy to enhance Kerr constant is to increase pitch length, i.e., to shift the Bragg reflection to a longer wavelength, say ~ 750 nm. However, this approach has some tradeoffs in response time and contrast ratio because higher-order Bragg reflections still occur in the visible region.

The response time of a polymer-stabilized BPLC material is related to the LC parameters as [29]:

$$\tau \approx \frac{\gamma_1 P^2}{k(2\pi)^2}, \quad (5)$$

where γ_1 is the rotational viscosity of the BPLC system, which is closely related to the viscosity of the LC host and the chiral dopant. A low viscosity LC host is always favorable from the response time viewpoint. However, there are compromises between large Kerr constant and fast response time. For example, large $\Delta\epsilon$ is helpful for boosting Kerr constant, but its viscosity is usually large. Similarly, increasing pitch length helps to enhance Kerr constant, but it will slow down the response time as Eq. (5) indicates. All these factors should be taken into consideration in order to develop a high Kerr constant BPLC while remaining the fast response time feature. For example, Chisso JC-BP01M has an extraordinarily high Kerr constant (~ 13.7 nm/V²) because its host LC has $\Delta\epsilon \sim 94$ and $\Delta n \sim 0.17$ [30]. Meanwhile, the clearing temperature of Chisso JC-BP01M is $\sim 70^\circ\text{C}$ and the response time in an IPS cell is ~ 1 ms at $\sim 30^\circ\text{C}$.

3.2 Chiral dopants

Chiral dopants induce twist in blue phases. Blue phases only appear as the chirality ($q_0 = 2\pi/P$) exceeds a certain value. To increase chirality, we can either increase the chiral dopant concentration or employ a chiral dopant with a high helical twisting power (HTP). Since the solubility of a chiral dopant limits its maximum concentration, it is preferred to use a high HTP chiral dopant. For example, Merck developed a chiral dopant with HTP $\sim 170\mu\text{m}^{-1}$, which to our best knowledge has the highest helical twisting power [31].

Another important parameter to consider for selecting a chiral dopant is the melting point. For example, CB15 shown in Fig. 4 has a very low melting point $\sim 4^\circ\text{C}$. Therefore, after mixing with the LC host, the clearing temperature of the mixture drops substantially as compared to the LC host. To make a wide temperature BPLC, the chiral dopant should have a higher melting point while keeping good solubility. The solubility of chiral dopant in a nematic LC host is affected by several factors, such as the melting point and heat fusion enthalpy of the chiral dopant. High melting point and large heat fusion enthalpy are less favorable because they would lead to limited solubility. As shown in Fig. 4, the chiral dopant ISO-(6OBA)₂ has a melting point of 90°C , HTP $\sim 35\mu\text{m}^{-1}$ (which depends on the LC host) and its solubility is ~ 10 wt%. On the other hand, ZLI-4572 has a similar HTP to ISO-(6OBA)₂, but its solubility is poorer because of its higher melting point.

3.3 Monomers

Monomers are essential in determining the stability of BPLC. Typically, a polymer-stabilized BPLC requires two types of monomers: mono-functional (EHA or C12A) and di-functional (RM257) monomers. The overall monomer concentration, as well as the ratios between the

two monomers needs to be optimized. We have investigated the effect of polymer concentration and composition [32]. We prepared a BPLC mixture consisting of 65 wt% Merck BL038 and 35 wt% chiral dopants (25% CB15 and 10% ZLI-4572). Two types of monomers (C12A and RM257), as well as a small amount of photoinitiator (~0.5 wt%) were added to the BPLC mixture. The concentration of C12A should be lower than 6% in order to observe blue phase in the precursor. To investigate the polymer effects, seven precursors with different monomer concentrations were prepared, as listed in Table 1. The total concentration of monomers varies from 9% to 15%, and the ratio between RM257 and C12A varies from 1:1 to 3:1. In-plane-switching cells with 10 μm electrode width and 10 μm electrode gap were employed to generate horizontal electric field so that phase retardation can be accumulated by a normally incident light. From Table 1, it is found that as the polymer concentration increases, the polymer network becomes more stable which in turn leads to faster response time and higher operating voltage. Once the overall polymer concentration is fixed, monomer ratio also affects the stability of polymer network. The 1:1 ratio is preferred since it gives a faster response time and less residual birefringence (not shown here).

Table 1. Operation Voltage, Hysteresis and Response Time of Seven Samples

Monomer Ratio Concentration	1:1			2:1			3:1		
	V_{on}	Hysteresis	τ (ms)	V_{on}	Hysteresis	τ (ms)	V_{on}	Hysteresis	τ (ms)
9%	157	4%	0.44	147	3%	0.68	148	3.5%	0.84
12%	176	3.5%	0.34	180	3%	0.54	179	3%	0.52
15%	N/A			$V_{\text{on}} > 200\text{V}$		0.30	N/A		

In addition to short pitch length and low viscosity described in Eq. (5), a strong polymer network is also helpful for reducing response time and suppressing hysteresis. As shown in Fig. 4, TMPTA is a tri-functional monomer, while the normally used EHA and C12A are mono-functional monomers. The crosslink between TMPTA and RM257 is much stronger, resulting in an increased elastic torque of the BPLC composite (which is favorable for response time) and decreased hysteresis. However, the downside is the increased operation voltage. Therefore, a delicate balance between operation voltage and response time needs to be taken.

Besides the material optimizations, photoinitiator and UV irradiation conditions also affect the performance of a PS-BPLC composite, such as photoinitiator concentration, the wavelength and intensity of UV light, exposure time, and curing temperature [33]. For example, a typical UV dosage for preparing polymer-stabilized BPLC composite is $\sim 3.6 \text{ J/cm}^2$ and the intensity varies from 1 mW/cm^2 to 20 mW/cm^2 [30,32]. The employed UV wavelength is usually $\sim 365 \text{ nm}$ and the curing temperature is near the chiral nematic to blue phase transition temperature [34]. A longer UV wavelength would penetrate to the LC cell more uniformly and produce more uniform polymer networks. This process is helpful for reducing hysteresis and residual birefringence.

4. Potential applications

The most attractive feature of polymer-stabilized BPLC is its fast response time, which makes it a strong contender for next-generation display technology. The sub-millisecond response time enables color sequential display using RGB LEDs, which in turn eliminates the spatial color filters. Consequentially, the optical efficiency and resolution density are all tripled. Other attractive features include intrinsic wide viewing angle because it is optically isotropic in the voltage-off state, no need for surface alignment layer, and cell gap insensitivity for IPS mode. The last two features are particularly attractive for fabricating large panel displays.

However, there are several technical challenges, such as operation voltage, hysteresis, stability, contrast ratio, and voltage holding ratio, that remain to be overcome before widespread applications can be realized. Tremendous progresses are being made recently. For example, besides the material optimizations that have been discussed in Sec. 3, device optimization also helps to reduce the operating voltage to ~10V so that amorphous silicon TFT addressing is enabled [35–37]. Hysteresis is related to the maximum electric field. Several approaches have been proposed to eliminate hysteresis [37,38].

The electric-field-tunable blue phase liquid crystals are also promising candidates for photonics application. The three-dimensional photonic structures with lattice constant several hundred nanometers give rise to selective Bragg reflection, which can be tuned by an electric field. Based on this electrostriction effect, tunable color devices have been experimentally demonstrated [13,17]. For example, in [13], the wavelength is tuned continuously from 572 nm to 506 nm with decay time in the range of tens of millisecond. The electrically tunable colors are suitable for optical filter devices and reflective display applications. Blue phases also find applications in lasing [39,40]. In a blue phase lasing device, a BPLC is doped with a small amount of dye, which emits light once excited. The Bragg reflection provides feedback so that laser emission can be detected.

Polymer-stabilized BPLC has negligible lattice distortion under electric field so the color change is not as obvious as pure blue phases. However, the refractive index change caused by Kerr effect can also be utilized in photonics applications, such as tunable phase gratings [41] and tunable micro-lenses [42–44].

5. Conclusion

Both pure blue phases and polymer-stabilized blue phases exhibit three-dimensional cubic structures, which results in selective Bragg reflections. For pure blue phases, the reflection band can be tuned by electric field. For polymer-stabilized BPLCs, electric field effects are governed by Kerr effect, which leads to refractive index changes and induced birefringence. Therefore, blue phases are particularly attractive for display and photonics applications where fast response time is needed.

Acknowledgments

The authors are indebted to Yuan Chen for help in preparing the manuscript and Industrial Technology Research Institute (ITRI, Taiwan) for financial support.